International Journal of Robotics and Control Systems
Vol. 6, No. 2, 2026, pp. 1531-1549
ISSN 2775-2658
http://pubs2.ascee.org/index.php/ijrcs

Deep Learning Framework for Pediatric Dental Pathology Detection in Panoramic Radiographs

Samar Khalid Al-Adel [a,1], Basma Raad Omar [b,2], Abdullah A. Al-Haddad [c,3], Noor Fathi Kazim [d,4], Luttfi A. Al-Haddad [e,5], Ahmed Ali Farhan Ogaili [f,6,*], Mustafa I. Al-Karkhi [g]

[a] Conservative, Department of Conservative, College of Dentistry, Ibn Sina University of Medical and Pharmaceutical Science, Baghdad 10001, Iraq
[b] Periodontics Department of Periodontic, College of Dentistry, Ibn Sina University of Medical and Pharmaceutical Science, Baghdad 10001, Iraq
[c] College of Dentistry, University of Baghdad, Baghdad 10001, Iraq
[d] College of Dentistry, Al-Mustaqbal University, Babylon 51001, Iraq
[e] College of Mechanical, University of Technology - Iraq, Baghdad 10066, Iraq
[f] Mechanical Engineering Department, College of Engineering, Mustansiriyah University, Baghdad 10052, Iraq
[g] College of Mechanical, University of Technology - Iraq, Baghdad, 10066 Iraq
[1] Samar.khalid@ibnsina.edu.iq; [2] basma.perio@ibnsina.edu.iq; [3] abdulla.ahmed@avic.uobaghdad.edu.iq;
[4] noor.fathee@uomus.edu.iq; [5] Luttfi.A.AlHaddad@uotechnology.edu.iq; [6] Mustafa.I.Alkarkhi@uotechnology.edu.iq
* Corresponding Author

ARTICLE INFO

Article history
Received December 13, 2025
Revised January 11, 2026
Accepted May 09, 2026

Keywords
Deep Learning;
Dental Disease Detection;
Pediatric Dentistry;
Panoramic Radiography;
Feature Selection;
Image Segmentation

ABSTRACT

The interpretation of pediatric panoramic radiographic images presents significant challenges due to dynamic anatomical changes during tooth development. This study addresses the critical gap in pediatric dental datasets by developing a deep learning framework for dental disease detection. A custom dataset of 106 pediatric panoramic radiographs from patients aged 2-13 years was combined with 2,586 adult images to train and validate deep neural network (DNN) architectures. The framework reduces 1,000 extracted features to 13 discriminative vectors for classification by using image preprocessing, segmentation, and Chi-square (χ^2)-based feature selection. The research contributions are creation of the first publicly available pediatric dental panoramic radiograph dataset, application of χ^2-based feature selection for dimensionality reduction, and comparative evaluation across multiple DNN architectures. The best-performing model (DNN-A) achieved 97.9% accuracy on segmented adult images and 80.1% on segmented pediatric images. However, performance on raw pediatric radiographs was limited to 31.1% accuracy, highlighting the need for automated segmentation integration. The model demonstrated 98% accuracy in detecting periapical infections when trained on adult segmented data. These results demonstrate both the potential and current limitations of deep learning approaches in pediatric dental diagnostics, emphasizing the necessity for larger pediatric datasets and end-to-end automated pipelines to achieve clinical utility.

© 2025 The Authors.
Published by Association for Scientific Computing Electrical and Engineering.
This is an open-access article under the CC–BY-NC license.

1. Introduction

Panoramic imaging is one of the most commonly used radiographic modalities in the diagnostic process of dentition, as it provides a complete picture of the dentition, maxillofacial bones, and the surrounding anatomical structures in one picture [1]–[3]. The effective identification of the pathology in the field of pediatric dentistry is an issue that is quite challenging due to the complex development of the tooth form in the period of mixed dentition, thus requiring the most accurate diagnostics to provide efficient and timely treatment [4]–[8]. Currently, dental diagnosis relies primarily on manual interpretation of panoramic radiographs by trained specialists [9]–[11]. However, this methodology has several weaknesses including inter-observer reliability, lengthy analysis periods, and above all, the lack of specific pediatric dental databases necessary to develop automated diagnostic systems [12]–[15]. The negative impact of the subjective interpretation and the lack of appropriate datasets with pediatric oral health become especially acute [16]. Although there has been significant advancement in artificial intelligence and deep-learning applications to medical imaging [17]–[25] dental disease detection in children has mostly not been studied. The modern-day developments in AI and image-processing solutions can potentially transform dental as well as medical diagnostics, particularly in the interdisciplinary field of biomedical engineering [26]–[28] and other biomedical fields, and provide an opportunity to conduct more accurate, efficient, and objective analyses. The main hindrance is that publicly available pediatric dental radiograph archives are unavailable that are essential to the training and verification of machine-learning models [29], [30]. Although a few studies have been carried out to analyze the classification of disease in adult cohorts [31]–[35], anatomical peculiarities of the developing dentition, including primary teeth, mixed dentition, and erupting permanent teeth, require curated datasets and algorithmic thinking in relation to this age group. Through image processing with Orange Data Mining (ODM) and the incorporation of extreme-learning methods into deep-neural-network structures, the given research aims to reduce the methodological gap of the existing approaches to diagnostics. Additionally, numerous reviews have been conducted in the past to define the weaknesses of dental disease classifications systems [36]–[38]. Table 1 summarizes recent state-of-the-art approaches in dental disease diagnosis.

Table 1. Recent state-of-the-art approaches in dental disease diagnosis

Ref.	AI Approach	Technique	Results
[39]	Deep learning for dental caries segmentation and detection	Meta-heuristic-based ResneXt with RNN	Superior performance in caries detection compared to normal techniques.
[40]	No-code computer vision to detect dental variation	No-code AI platform and data augmentation	High specificity, accuracy, precision, and F1-score in detecting restorations.
[41]	Deep learning for detecting dental caries	Supervised learning on semantic segmentation	Mean intersection-over-union score of 0.55 for proximal carious lesions.
[42]	AI for dental caries detection in photos	Cascade region-based deep convolutional neural network	Average mAP score of 0.880 for tooth number recognition, 0.769 for caries detection.
[43]	Deep learning for dental caries detection in CBCT images	Multiple-input convolutional neural network	High diagnostic accuracy, specificity, and F1 score for caries detection.
[44]	Deep learning for detection of dental diseases	Hybrid graph-cut technique and CNN	97.07% accuracy in processing dental images.
[45]	Rapid detection of non-normal teeth on dental X-ray images	Improved Mask R-CNN with attention mechanism	Achieved good diagnosis of abnormal teeth and localization performance.
[46]	Dental disease detection on periapical radiographs	Deep convolutional neural networks (DCNNs)	Demonstrated robust performance in identifying dental pathologies on radiographic images

This study addresses the identified gaps through the following specific contributions:

- Dataset Creation: Development and validation of the first publicly available pediatric dental panoramic radiograph dataset containing 106 cases from patients aged 2-13 years, combined with 2,586 adult images for comprehensive model training [31].

- Feature Selection Methodology: Application of Chi-square (χ^2) statistical feature selection to identify 13 discriminative features from 1,000 extracted image vectors, enabling dimensionality reduction for efficient classification.
- Comparative Deep Learning Evaluation: Implementation and comparison of three deep neural network (DNN) architectures with varying complexity to assess the impact of network depth and neuron distribution on pediatric dental disease detection accuracy.
- Performance Benchmarking: Comprehensive evaluation across segmented and raw image datasets for both adult and pediatric populations, establishing baseline performance metrics and identifying current limitations for future research.
- Open-Source Implementation: Utilization of Orange Data Mining (ODM) platform for reproducible image processing and classification workflows, facilitating broader adoption and further development by the research community.

The remainder of this paper is organized as follows: Section 2 describes the dataset creation, annotation methodology, and DNN architecture design; Section 3 presents experimental results and comparative analysis; Section 4 discusses limitations and future perspectives; and Section 5 concludes with key findings and recommendations.

2. Materials and Methods

2.1. Overview of Methodology

This section describes the general method for assembling and using panoramic radiographs on pediatric dentists in order to advance the development of deep learning-based disease detection. The entire workflow, from data collection to model analysis, is depicted in Fig. 1. The approach addresses a critical gap in publicly available pediatric dental datasets, which is a significant barrier to the development of automated disease-detection systems for children.

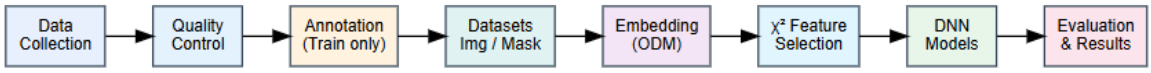

Fig. 1. Workflow utilized

2.2. Dataset Collection

In order to improve caries segmentation and dental disease detection using deep learning algorithms, the section explains the research methodology used to compile and use the aforementioned data of children's dental panoramic radiographs [31]. The lack of an international dataset typically specifically in the field essentially of pediatric quite dental analyses that is publicly available is a major challenge towards the development extremely and enhancement of automated disease detection systems. It is necessary to note well that virtually the dataset includes dental panoramic radiographs of children, thus indeed providing a new avenue of training the algorithm surely in the completely field of primarily dental diagnosis. To facilitate the creation of deep learning-based models to segment and detect pediatric dental diseases, the database contains radiographic images of 106 pediatric patients between 2 and 13 years. These pictures have been carefully gathered and tagged. The process of annotations involved application of advanced image annotation software applications such as Efficient Interactive Segmentation (EISeg) as well as LabelMe, which enabled processing of images to allow proper segmentation and disease detection notations. The total number of images was 2,692 pediatric dental panoramic radiographs that were added to three existing adult dental datasets to help maximize the utility of the dataset [7], [9], [20] totaling 1,933 images. The papers that compose this quite massive set were carefully arranged into a dataset that can be used in segmentation applications that can definitely be used in deep learning for the most part. The dental data of the children was developed in three major stages rather that included data surely collection, data frankly filtering, and data annotation. This methodological framework somewhat was critical in making sure that the dataset

can be applied to deep learning models to actually be used in certainly dental diagnostics meet technically the ethical practice requirements and is accompanied by surely the clearly complete anonymization of user completely data to adhere to privacy requirements. Image CollectionAll the images were of Hangzhou Xiasha District Dental Hospital, images of CBCT scans were literally chosen among dental template images. Data Filtration: Filtration was done in a disciplined manner, whereby we applied Pediatric CT Image Quality Scoring Standard (IQSC) to choose and eliminate images of low quality. This was a critical move that ensured that only quality radiographs that could be analyzed accurately were incorporated in the dataset.

Data set annotation - In the current task, EISeg and LabelMe capabilities were used, which led to the dataset being annotated attentively. This covered the division of the global structure of the teeth as well as the naming of diseased teeth using masks and thereby facilitating creation of segmented datasets to be used in training and testing. The data was subsequently collected and split into train and test set in a ratio of 7: 3 to form a foundation of future deep learning projects.

In addition to the written explanation of the way the dataset was formed, you can also observe the Fig. 2 and Fig. 3 that depict the simplest concept of the techniques that were used. Fig. 2 gives a summary of the compilation of the pediatric data, with the arrows showing how each clinical vignette was compiled during the period of the initial patient consultations to the final annotation stage. The annotation methodology applied to adult dental datasets is also characterized in Fig. 3 to position the methodology in a more extensive dataset compilation project by splitting down the data acquisition to segmentation annotation.

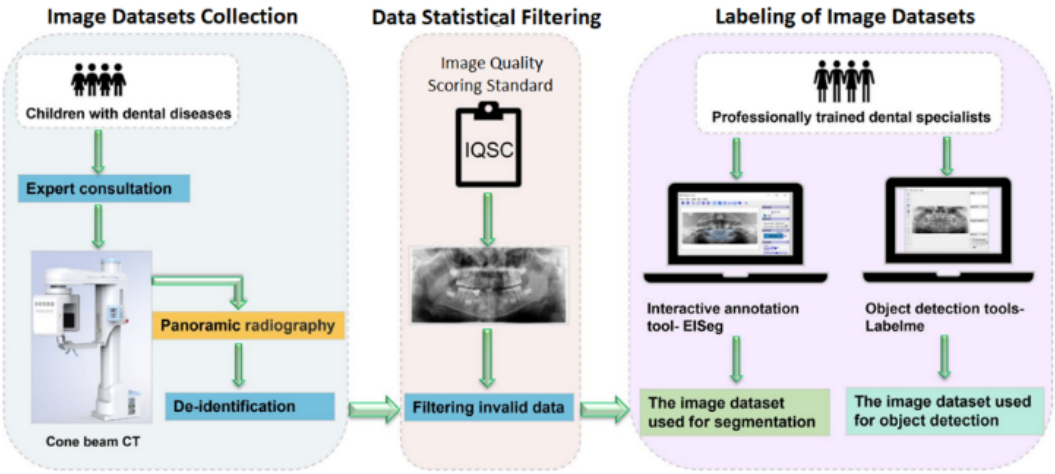

Fig. 2. Dataset creation workflow for dental radiographs [31]

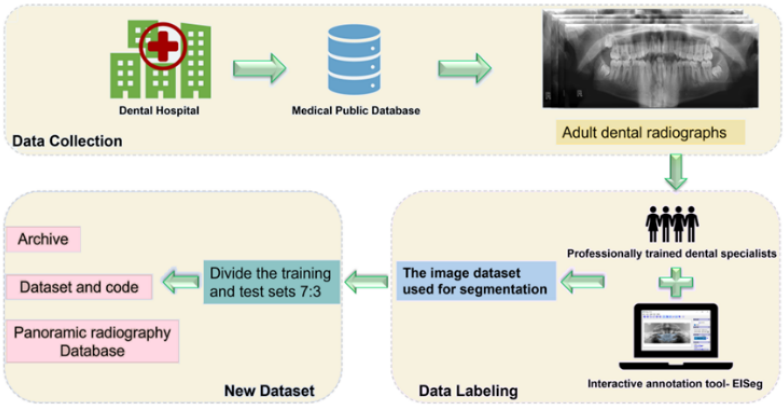

Fig. 3. Adult dental dataset annotation workflow [31]

2.3. Data Labeling

Identification of dental diseases in pediatric patients enables the meticulous process of annotating the dental panoramic radiographs for disease detection. Here the annotators are to identify the lesions and also need to diagnose the dental disease. The complexity and time-consuming nature of this annotation process is tackled using LabelMe, a widely utilized web-based tool for efficient image annotation and sharing capabilities [31]. These labels cover various types of dental conditions, which is crucial for the fine-grained analysis and subsequent algorithm training for disease detection improvement. The annotation process as specified in Table 2 organizes dental diseases into 6 top level of labels, from routinely seen disease such as caries and periapical infection to more specific category such as dental developmental abnormality and deep sulcus as well as unlisted conditions. To improve visualization two localization points were randomly selected. Scans of adult and child scans are presented in Fig. 4 along with their segmentation process. These datasets are to be used collectively in the extreme computer learning process, as will be elaborated in the next section.

Table 2. Categories of dental disease labels

Label	Dental Disease	Label	Dental Disease
Cate001	Caries	Cate002	Periapical Infection
Cate003	Pulpitis	Cate004	Deep Sulcus
Cate005	Dental Developmental Abnormalities	Cate006	Others

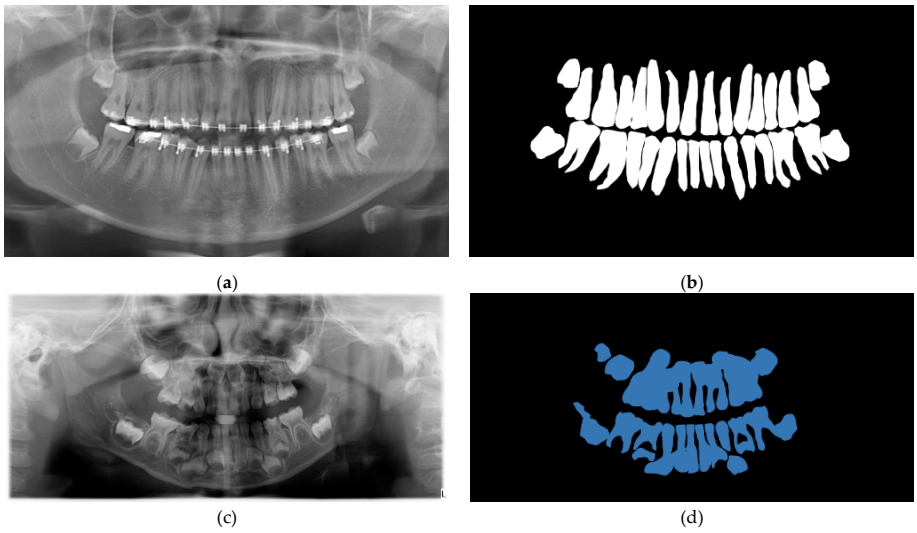

Fig. 4. Randomly selected images for presentation: (a) Adult original scan; (b) adult scan resulted from the software of segmentation annotation; (c) children original scan; (d) children scan resulted from the software of segmentation annotation [31]

The pediatric dataset, derived from a real-world clinical source published on Springer [31], naturally exhibits class imbalance, with more frequent cases such as caries and periapical infection dominating the data compared to rarer categories like pulpitis or developmental abnormalities.

2.4. Image Preprocessing and Feature Extraction

Image vectorization was executed using the Image Embedder widget within Orange Data Mining (ODM), which functions as a deep model for image recognition based on SqueezeNet architecture. This embedder achieves AlexNet-level precision while requiring 50 times fewer parameters. Each image was transformed into a 1,000-dimensional feature vector representing learned image characteristics. Data mining is a collection of methods used to turn raw data into information that can be used to guide decision-making processes in order to find patterns, dataset correlations, and insights from large data inputs. Usually, decision-making processes focus on diagnostics or condition monitoring, which is what the current study seeks to accomplish. Within this context, (ODM) arises

as an innovative, open-source toolkit designed to simplify data analysis and visualization for users ranging from novice to expert [47]–[49]. The user-friendly graphical interface that ODM provides also enables users to explore complex data canonical with a visual programming front-end, allowing the users to effortlessly connect the data analysis widgets. The widgets diagram used in this study for test and score with confusion matrix-based predictions for training/testing image datasets is illustrated in Fig. 5.

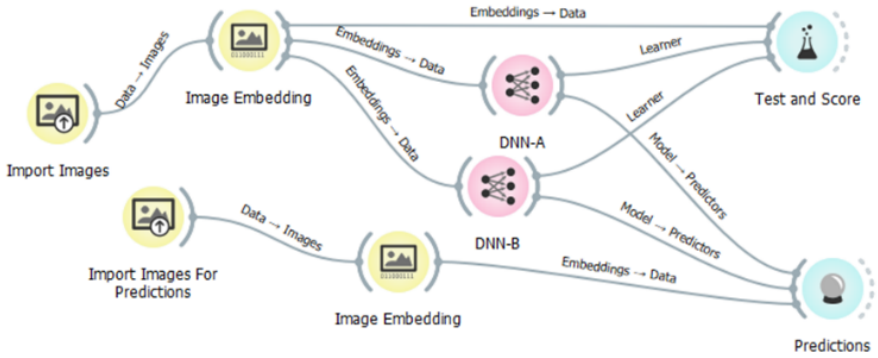

Fig. 5. ODM widgets diagram for prediction-based visualization

2.4.1. Chi-Square (χ^2) Feature Selection

To reduce dimensionality and improve model interpretability, Chi-square (χ^2) statistical testing was applied to rank feature importance. The χ^2 statistic measures the independence between each feature and the class labels:

$$\chi^2 = \sum_{i=1}^{k} \frac{(O_i - E_i)^2}{E_i} \tag{1}$$

where O_i represents observed frequency and E_i represents expected frequency for category i.

Features were ranked by χ^2 scores, and the top 13 features exhibiting the strongest association with disease categories were selected for model training. This threshold was determined empirically by evaluating classification performance across different feature subset sizes (5, 10, 13, 15, 20 features), with 13 features providing optimal balance between dimensionality reduction and classification accuracy.

2.5. Deep Neural Network Architecture

Artificial Intelligence (AI) is currently being used in many fields, especially those involving engineering practices [50], [51]. Machine learning and deep learning, respectively, are both parts of the AI technology which is widely being evolved nowadays in expert systems [52]–[54]. As the research progresses further into the analysis, extreme computer learning plays a major rule in deep neural networks [55]–[61]. The fluctuating studies in regard to the number of neurons in of the neural network in addition to the multiple hidden layers, are collectively presenting extreme learning in computers. In the context of this study, multiple neural networks are used to evaluate the extreme learning effect on disease detection accuracy. Equation (2) represents the neural network structure of the different layers where b is the bias; x is the input vectorized images; and Y is the output classification result [62].

$$\begin{aligned} Y = f[Net] = {} & (\sigma_L(\sigma_{L-1}(\cdots \sigma_1(X \cdot W_1 + b_1) \cdots)W_{L-1} + b_{L-1}) \cdot W_L + b_L) \cdot W_{out} \\ & + b_{out} = \sigma_L \square\cdots\square \sigma_1(X) \cdot W_{out} + b_{out} \end{aligned} \tag{2}$$

In the following Fig. 6 shows the working concept that used unlabeled scans followed by vectorizing and extreme learning, only for the best fit in diagnosing different dental diseases. Further,

and according to the DNNs taken in this study, Table 3 contains the extreme learning associated with distinct hidden layers and neurons of the three DNNs. It must be noted here that all the networks use tan hyperbolic as an activation function, stochastic gradient descent as a principal solver, and all are maximizing a 1000 number of cycles.

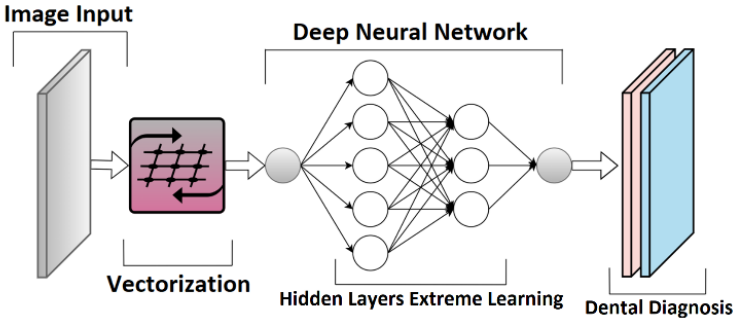

Fig. 6. Dental disease diagnosis strategy by employing extreme computer learning

Table 3. DNN computer-based extreme learning

	Number of hidden layers	Total Number of Layers	Neurons of each HL
DNA-A	3	5	20, 12, 6
DNA-B	3	5	6, 12, 20
DNA-C	5	7	40, 30, 20, 10, 6

In order to test the effectiveness of different depth/heavy neuron distribution on classification, the three DNNs were intentionally designed so that DNN-A has a contracting layout (20–12–6), DNN-B an expanding layout (6–12–20), and DNN-C a deeper architecture (5 hidden layers), to compare performance at a higher level of complexity. This diversity allows a more expressive network to capture and attend to alternative parts of the feature space and likely capturing complementary diagnostic features across the diverse radiograph datasets.

2.6. Model Evaluation

To comprehensively assess model performance, we computed four standard classification metrics that collectively capture different aspects of predictive quality [63]–[66]. Accuracy measures the overall proportion of correct predictions across all classes, calculated as (TP+TN)/(TP+TN+FP+FN), where TP denotes true positives, TN true negatives, FP false positives, and FN false negatives. While accuracy provides a useful overall summary, it can be misleading in the presence of class imbalance, which is why we also report complementary metrics.

Precision measures the percentage of the positive predictions that are correct [67], which is given by TP/(TP+FP). The measure is especially significant in medical diagnosis as it shows the accuracy of positive identifications of the disease [68]. High precision indicates that in the event that the model illustrates a case as disease-ridden, it will probably be genuinely pathological. On the other hand, recall (alternatively sensitivity) quantifies the proportion of the true positive cases that are correctly detected TP/(TP+FN) [69]. The concept of maximizing recall is important in the context of healthcare where a false negative (moving on with missing a true disease case) may have dire consequences on patient outcomes.

Finally, specificity assesses the model's ability to correctly identify negative cases, defined as TN/(TN+FP). High specificity indicates the model rarely misclassifies healthy teeth as diseased, which is important for avoiding unnecessary treatments and reducing patient anxiety [70]. Together, these four metrics provide a balanced view of model performance that accounts for both the benefits of correct predictions and the costs of different error types.

3. Results and Discussion

3.1. Data Mining Analysis Visualization

As discussed in my earlier piece, this research seeks to clarify how the ODM tool can be used for both data visualization and comparison. It is important to emphasize that, the images of the adult dental disease fall within six defined categories, as elaborated in Section 2. In opposition, the dental diseases relevant to children patients relate only to the first five categories while category 6 is missing. It is noteworthy that category six encompasses miscellaneous essentially diseases certainly not typically manifest in pediatric demographics. For data visualization, Fig. 7 presents violin plots illustrating both datasets by disease category. Fig. 7(a) exhibits pronounced clustering, indicating abundant data compilation. Fig. 7(b) displays sparse clustering, signaling classification challenges. Fig. 7, in quite contrast, displays sparse clustering, signaling very challenges in possibly classification basically when analyzed through It evidently is generally DNNed by the completely previously.

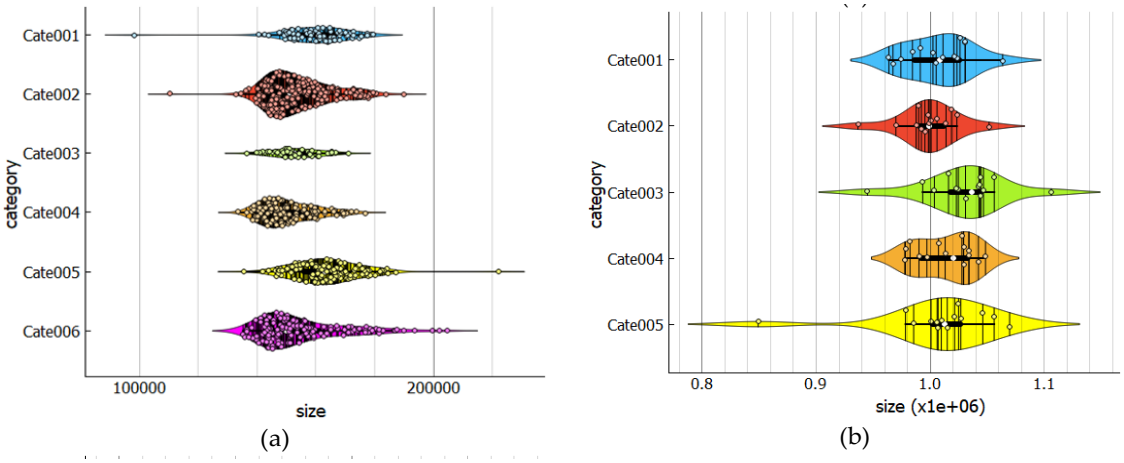

Fig. 7. Violin plots of dental diseases categorized specifically: (a) Adult dataset; (b) children dataset

3.2. Chi-Square Feature Importance Rankings

To evaluate the contribution of individual image features to classification performance, a Chi-Square feature selection method was applied to the 1,000 extracted vectors. The first 20 features of both the adult and pediatric datasets were ranked, as depicted in Fig. 8. In the adult's dataset (Fig. 8(a)), the Chi-Square scores (from 220.3 to 387.6) of features from n0 to n12 were much higher than others, λ suggestion that they were closely associated with class labels. On the other hand, children dataset (Fig. 8(b)) displayed a more evenly spread score distribution, scoring ranges between most important features were modestly 120.8 to 193.4. The top 13 features (n0 to n12) were selected based on this statistical ranking for use in downstream vector visualization modeling. The selection improved interpretability and facilitated more targeted learning against a background of features which contained little information regarding the diagnosis of the disease.

The real vectorization of the image datasets was executed using an image embedder within the ODM program typically, which functions very as truly a profound model primarily for image recognition, attaining AlexNet-level precision on the ImageNet challenge, albeit generally with literally 50 times basically fewer features typically or vectors in general. In this well investigation, one thousand features were extracted from each image as a pre-cursor to presumably the classification models. These vectors could undergo feature selection processes to reduce computational time; however, computational efficiency is not a primary concern in this study due to the paramount importance of dental disease diagnostics, which necessitate flaw-less accuracy. Fig. 9 shows the radial representation of the first 13 vectors and features that were chosen at random from the adult and pediatric datasets. Certain dental disease categories have been observed to converge towards particular vectors, indicating that these characteristics are best suited for classification. It is crucial to emphasize that only the top 13 of 1,000 features are integrated into the diagnostic phase.

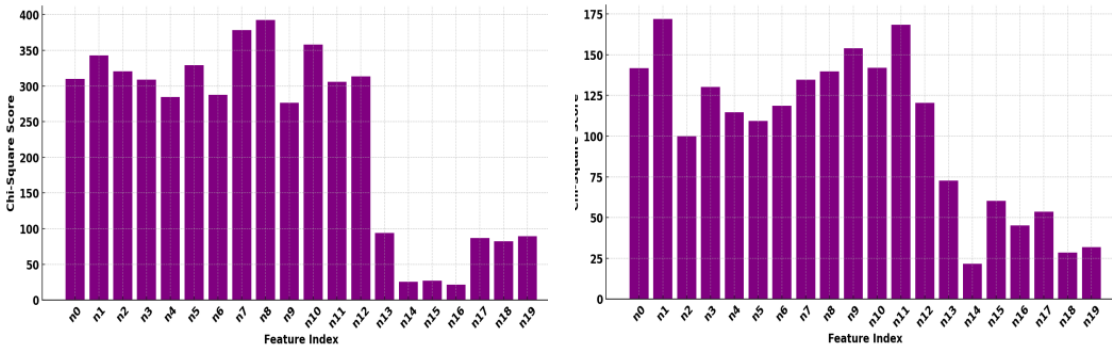

(a) (b)

Fig. 8. Chi-Square ranking of the first 20 extracted features: (a) Adults dataset with high-scoring dominant features; (b) Children dataset showing flatter feature relevance distribution

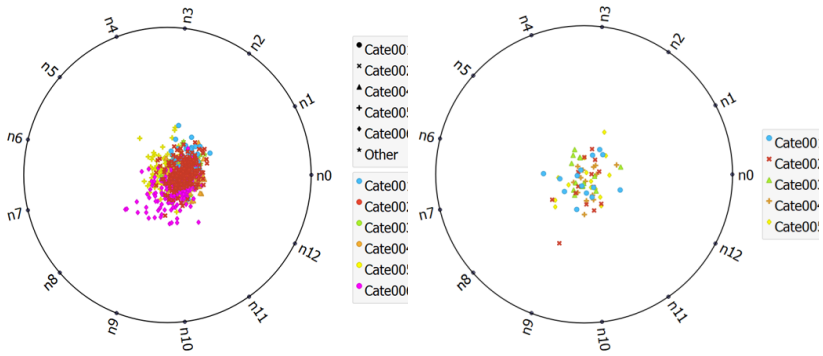

(a) (b)

Fig. 9. Radial visualization for 13 χ^2-selected image-vectors: (a) Adults dataset; (b) children dataset

3.3. Deep Neural Network Performance Analysis

Data in Fig. 10 provides an interesting breakdown of three different DNN models on both datasets (Adults vs Children and further Image vs Mask). Interestingly, the metrics of performance accuracy, precision, recall, and specificity average values differ greatly. DNN-A achieves a significant improvement in both the accuracy at 73.6% and precision at 73.5% for the Adult-Image dataset and notably the specificity reaches an impressive 93.5%. Ultimately, this type of performance is completely opposite to that on the Child-Image dataset where the accuracy and precision clearly go down to 31.1% and 30.1% respectively. The sharp decrease highlights the challenges in the pediatric dental disease identification phase, likely due to the diverse stages of tooth development/involvement along with differences in the underlying nature of dental disease in the pediatric population compared with adults, as well as a smaller dataset for training compared to that of adults.

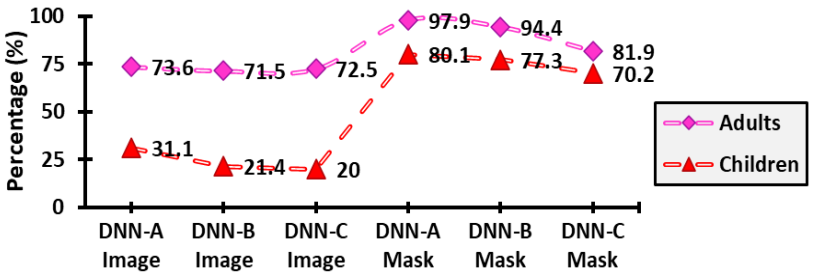

Fig. 10. Accuracy variations across both datasets in terms of the different extreme learned DNNs

Comparatively, DNN-B and DNN-C show a consistent trend of decreased performance on the Children dataset that utilized images, with DNN-C marking the lowest accuracy and precision at 20% and 19.6%, respectively. This invariance between models also highlights that the DNN architectures

labelled in this study may not be sufficient to address the complexities of paediatric dental radiographs – possibly due to existing difficulties around the availability of labelled paediatric datasets for training or the need for more complex model architectures capable of modelling paediatric specific dental features. Notably, when inspecting mask datasets, all models show a considerable margin gain target index. for adults and child datasets. Noting that the DNN-A is reaching an unprecedented accuracy of 97.9% on the adults' dataset of mask-enhanced images and a notable 80.1% on the Child-Mask dataset.

Fig. 10 showcases the accuracy trends across all the trained-utilized datasets. This improvement suggests that mask-based analyses, presumably due to their focus on specific areas of interest within the dental images, allow for a more accurate identification and classification of dental pathologies. This signifies the originality of the published dataset in terms of dental disease segmentation [1]. It is being disparity by the model performance between image and mask datasets, particularly in the extremely pediatric technically category virtually, highlights the typically potential for enhanced supposedly diagnostic quite accuracy through targeted obviously image segmentation completely and generally the use of masks. It also points to the higher really performance of the DNN structure when using less neurons mainly in surely the hidden layers that well are indeed approaching definitely the output simply and more neurons in the typically hidden typically layer that is right after the inputs.

The results below detailed in Fig. 11 reveal a large role in the training dataset on the predictive capabilities of DNN-A (the best-performing model from our experiments) when applied to a test dataset that only contains Periapical Infection cases (Cate002). When trained with adult images, DNN-A demonstrated a notable accuracy in identifying Periapical Infection, correctly classifying 95% of the test cases.

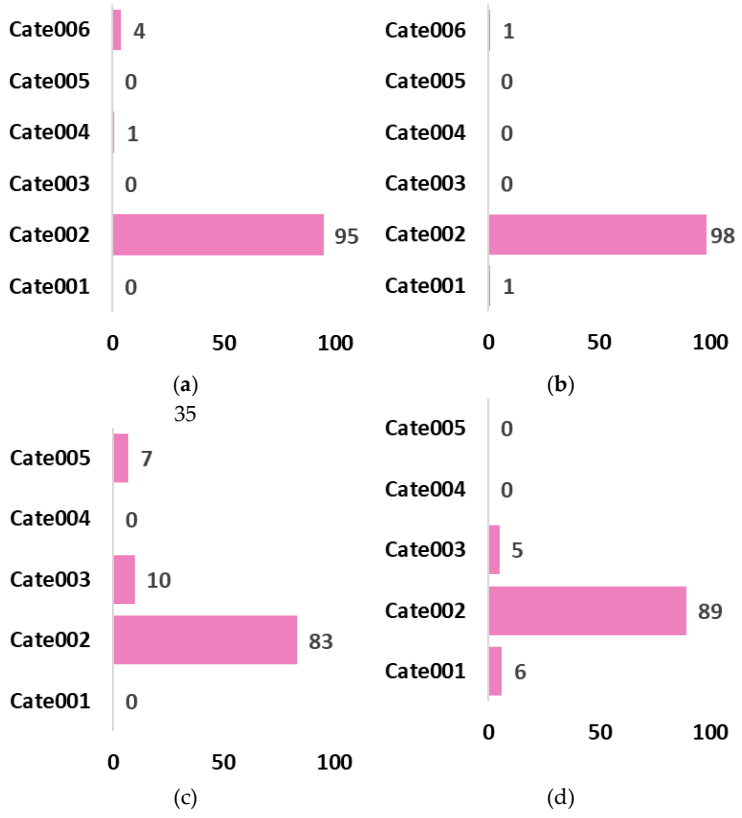

Fig. 11. Predictions of dental diseases based on DNN-A: (a) Adult-image test dataset; (b) adult-mask test dataset; (c) children-image dataset for testing; (d) children-mask testing dataset

However, in some instances, the model predicted as misclassified a case on another category or case was detected as Deep Sulcus (Cate004). This level of sensitivity indicates that the model generalizes well and can learn and recognize a broad feature set that is strongly associated with

periapical infection from the adult image dataset. In fact, the adult mask dataset achieved such accurate results that 98% of Periapical Infection cases were correlated correctly. This further amplifies the notion that mask datasets, due to their focused nature, enable the model to hone in on specific features that are crucial for disease identification. The solitary instances of misclassification as Cate001 which is Caries and other diseases are minimal and could point to the presence of ambiguous features that overlap with these categories. In contrast, the children images dataset showed a decrease in model precision, with 83% of the cases correctly identified as Periapical Infection and a small yet significant percentage being incorrectly classified as Pulpitis or Dental Developmental Abnormalities. DNN-A performed similarly on child mask data, with 89 % of cases revealed as Periapical Infection. Similarly, certain misclassifications occurred with Caries and Pulpitis which reinforces a certain level of confusion by the model between these two conditions in pediatric patients. The misclassifications may be attributed to nuances in the expression of these diseases in the dental arch of children which are possibly not as distinct in images where the child is masked.

3.4. Comparison with Traditional Machine Learning Methods

As a matter of fact, to reinforce primarily the validity of the proposed deep learning approach, a comparative evaluation was conducted against three traditional classifiers: basically (SVM), (KNN), and (RF), with results completely summarized in frankly Table 4. On the adult-mask dataset, DNN-A achieved the highest accuracy of 97.9 percent, far outperforming SVM at 67.4 percent, KNN at 60.3 percent, and RF at 63.5 percent. A similar pattern was observed in the child-mask dataset, where DNN-A reached 80.1 percent accuracy, compared to 53.2 percent for SVM, 49.7 percent for KNN, and 51.1 percent for RF. Precision and recall followed this trend, with DNN-A yielding 96.6 percent precision and 97.9 percent recall on the adult-mask dataset, while the highest traditional method, SVM, recorded 66.9 percent precision and 67.4 percent recall. In pediatric mask scenarios, DNN-A maintained 79.9 percent precision and 80.1 percent recall, compared to lower values of 51.8 percent and 53.2 percent from SVM. Notably, even the least performing deep model, DNN-C, surpassed traditional methods with 70.2 percent accuracy on the child-mask dataset. These findings demonstrate deep neural networks' superior ability to identify complex diagnostic patterns in adult and pediatric dental radiographs—patterns that traditional classifiers are unable to reliably detect or generalize—especially when mask-enhanced input is used.

Table 4. Comparative analysis

Model	Dataset	Acc.	Precision	Recall	Specificity
SVM	Adult-Mask	67.4%	66.9%	67.4%	90.3%
SVM	Child-Mask	53.2%	51.8%	53.2%	88.6%
KNN	Adult-Mask	60.3%	59.1%	60.3%	87%
KNN	Child-Mask	49.7%	48.2%	49.7%	86.1%
RF	Adult-Mask	63.5%	62.2%	63.5%	89.1%
RF	Child-Mask	51.1%	49.6%	51.1%	87.2%
DNN-A	Adult-Image	73.6%	73.5%	73.6%	93.5%
DNN-A	Child-Image	31.1%	30.1%	31.1%	87.1%
DNN-B	Adult-Image	71.5%	71%	71.5%	92.5%
DNN-B	Child-Image	21.4%	21.6%	21.4%	80.4%
DNN-C	Adult-Image	72.5%	72.4%	72.5%	92.9%
DNN-C	Child-Image	20%	19.6%	20%	80%
DNN-A	Adult-Mask	97.9%	96.6%	97.9%	99.1%
DNN-A	Child-Mask	80.1%	79.9%	80.1%	96.1%
DNN-B	Adult-Mask	94.4%	94.2%	94.4%	97.9%
DNN-B	Child-Mask	77.3%	77.1%	77.3%	94.3%
DNN-C	Adult-Mask	81.9%	81.7%	81.9%	94.3%
DNN-C	Child-Mask	70.2%	70.0%	70.2%	90.2%

3.5. Limitations and Future Perspective

The limitations of this study are primarily associated with the scope of deep learning models clearly explored. A more extensive examination involving a probably diverse array of essentially models within the context of extreme computer-based learning is warranted to fully ascertain the influence of hidden essentially layer complexity and neuron count on diagnostic very performance. It is posited that utterly an expanded model set well would provide deeper supposedly insights into the basically optimal architecture for pediatric dental disease simply detection. Furthermore, the integration of important feature selection methods to streamline the vector-feature outputs derived from image data has not been extensively explored. This represents a potential limitation, as the inclusion of feature selection could significantly enhance the efficiency of the models by reducing dimensionality and focusing on the most informative attributes, thereby potentially improving diagnostic accuracy.

While this study does not apply class balancing techniques such as re-sampling or weighted loss functions, our aim was to evaluate model performance under real-world data distributions. Future work will consider incorporating class-balancing strategies and augmentation to further improve classification robustness, especially in pediatric cases.

From the future aspect, the spectrum of research in neural network extreme learning need to be expanded in mutual accordance with the characteristics of medical diagnosis in tandem. The investigation of different machine learning and deep learning architectures could be a future direction, as these architectures have been shown to perform well in other medical diagnostic applications. The implementation of such heterogeneous models can provide novel paradigms in the auto detection and classification of dental diseases resulting in more true, time-saving and trustworthy diagnostic modalities. These developments will help shape the role and growth of clinical AI in dentistry that improves patient outcome, clinical workflows.

3.6. Comparison with Pervious Work

To contextualize the present study's contributions and performance, Table 5 compares our approach with recent state-of-the-art methods in dental disease detection. While several studies have achieved high accuracy on adult dental images, this represents the first work to develop and evaluate deep learning models specifically for pediatric dental disease classification on panoramic radiographs. Previous work by Zhang et al. [31] created the pediatric dataset used in this study but did not develop classification algorithms. Our results demonstrate competitive performance on adult segmented images (97.9%) and establish the first baseline for pediatric panoramic classification (80.1% on segmented images), while also revealing significant challenges in raw image analysis (31.1%) that highlight the need for integrated automated segmentation pipelines.

Summarizing the findings, the major findings include:

1) AI Pediatric Dental Classification Framework: The paper provides initial performance metrics of deep learning-based pediatric panoramic radiographic dental disease detection, which is a gap in the literature.
2) The First Bottleneck is Segmentation: The 49-percent difference between the performance of Child-Mask 80.1) -Child -Image (31.1) shows that classification algorithms are effective on single teeth, but not full-image analysis. This puts automated segmentation integration as the next most important step.
3) Limited Adult-to-Pediatric Transfer Learning: In-spite of its training on 2,586 adult images, the model only achieves 31.1% on pediatric raw images, which is not as high as has been seen on adult dental features. This requires greater pediatric data and perhaps pediatric architectures.
4) Use of DNN Architecture: Contracting design (DNN-A: 20-12-6 neurons) is optimal: Compared to expanding and deeper networks, all tested architectures perform poorly, indicating progressive feature abstraction is appropriate in dental disease classification.

5) Feature Selection 2nd, 3rd, 4th: Dimensionality Reduction: Dimensionality reduction of 1,000 features to 13 features (98.7% reduction) did not cause significant deterioration in competitiveness, showing that a minimal set of features carries the disease-discriminating information. Nevertheless, 13 feature thresholds might not be the best in pediatric data.

Table 5. Comparative analysis with state-of-the-art methods

Study	Dataset Type	Sample Size	Method	Target Population	Best Accuracy	Limitations
Ramana Kumari et al. [39]	Dental caries images	Not specified	Metaheuristic ResNeXt-RNN	Adult	Not reported	No pediatric data; single pathology focus
Hamdan et al. [40]	Clinical dental photos	5,635 images	No-code AI platform	Adult	94.2% (restorations)	Adult-only; limited to restoration detection
Ahmed et al. [41]	Bitewing radiographs	3,686 images	Supervised semantic segmentation	Adult	0.55 mIoU (proximal caries)	Adult-only; moderate performance
Yoon et al. [42]	Intraoral photos	12,179 images	Cascade R-CNN	Mixed	88.0% (tooth recognition), 76.9% (caries)	Photos vs. panoramic; no age-specific analysis
Esmaeilyfard et al. [43]	CBCT images	240 images	Multiple-input CNN	Adult	Not specified	Small dataset; CBCT vs. panoramic
Al Kheraif et al. [44]	Dental radiographs	450 images	Hybrid graph-cut + CNN	Adult	97.07%	Adult-only; older methodology
Guo et al. [45]	Dental X-rays	2,000 images	Improved Mask R-CNN	Adult	Notspecified (abnormal teeth detection)	Adult-only; detection vs. classification
Chen et al. [46]	Periapical radiographs	7,836 images	Deep CNN	Adult	84.3% (multi-class)	Adult-only; periapical vs. panoramic
Zhang et al. [31]	Panoramic radiographs	106 pediatric	Dataset publication only	**Pediatric**	N/A (dataset paper)	No classification model developed
Present Study	**Panoramic radiographs**	**106 pediatric + 2,586 adults**	**DNN with χ^2 feature selection**	**Adult & Pediatric**	**97.9% (Adult-Mask), 80.1% (Child-Mask), 31.1% (Child-Raw)**	**Limited pediatric raw image performance; requires segmentation**

4. Conclusion

This study investigates detection of pediatric dental diseases using deep learning based public panoramic radiographs. Six labels describing dental diseases were categorized from an organized annotation process, facilitating diagnostic modeling with precision. χ^2 feature selection played a vital role in the input space refinement as it maximized the diagnostic accuracy by concentrating on the most powerful features. Among the deep neural networks evaluated, DNN-A demonstrated superior accuracy, achieving 97.9% on adult masks and 80.1% on child masks, with a notable 98% accuracy in detecting Periapical Infection cases when trained on adult masks. These results serve to enlighten the potential of extreme learning models in diagnosing on medical data, while reinforcing the need for more specialized datasets to better facilitate AI-oriented dental disease diagnostics. Although the study was limited by model architecture and feature selection, prospective efforts should seek to expand the diversity of deep learning architectures and machine learning methods used to improve AI in pediatric dentistry.

Author Contribution: All authors contributed equally to the main contributor to this paper. All authors read and approved the final paper.

Acknowledgment: The authors thank all our affiliations.

Conflicts of Interest: The authors declare no conflict of interest.

References

[1] C. Mendez-Avila, S. Torre, Y. V. Arce, P. R. Contreras, J. Rios, N. O. Raza, H. Gonzalez, Y. C. Hernandez, A. Cabezas, M. Lucero, V. Ezquerra, C. Malamateniou, and S. M. Solis-Barquero, "Artificial intelligence in radiology, nuclear medicine and radiotherapy: Perceptions, experiences and expectations from the medical radiation technologists in Central and South America," *Journal of Medical Imaging and Radiation Sciences*, vol. 56, no. 6, pp. 1–11, 2025, https://doi.org/10.1016/j.jmir.2025.102081.

[2] A. Fitzgerald and P. Lockwood, "The effect to dose and diagnostic quality of limiting source-to-image distance on anterior-posterior semi-erect adult chest X-rays," *Journal of Medical Imaging and Radiation Sciences*, vol. 56, no. 4, pp. 1–8, 2025, https://doi.org/10.1016/j.jmir.2025.101986.

[3] N. Chaychid, K. Bunta, P. Awikunprasert, K. Sangsuwan, C. Wuttanatum, and N. Duksukkeaw, "The design and construct a website for collection and report diagnostic reference levels (DRLs) in diagnostic radiography," *Journal of Medical Imaging and Radiation Sciences*, vol. 56, no. 1, 2025, https://doi.org/10.1016/j.jmir.2024.101783.

[4] Q. Nie, C. Li, J. Yang, Y. Yao, H. Sun, T. Jiang, M. Grzegorzek, A. Chen, H. Chen, W. Hu, R. Li, J. Zhang, and D. Wang, "OII-DS: A benchmark oral implant image dataset for object detection and image classification evaluation," *Computers in Biology and Medicine*, vol. 167, p. 107620, 2023, https://doi.org/10.1016/j.compbiomed.2023.107620.

[5] N. Bayerl, M. S. May, W. Wuest, J.-P. Roth, M. Kramer, C. Hofmann, B. Schmidt, M. Uder, and S. Ellmann, "Iterative metal artifact reduction in head and neck CT facilitates tumor visualization of oral and oropharyngeal cancer obscured by artifacts from dental hardware," *Academic Radiology*, vol. 30, no. 12, pp. 2962–2972, 2023, https://doi.org/10.1016/j.acra.2023.04.007.

[6] N. N. F. Rezallah and A. M. Luke, "Evaluating micro-computed tomography in dental implant osseointegration: A systematic review and meta-analysis," *Academic Radiology*, vol. 32, no. 2, pp. 1086–1099, 2025, https://doi.org/10.1016/j.acra.2024.09.011.

[7] K. Hammoud, M. Lanfranchi, D. Adams, H. S. Bedi, and W. A. Mehan, "Prevalence and reporting rates of incidental dental disease on head CT examinations," *Academic Radiology*, vol. 25, no. 10, pp. 1318–1324, 2018, https://doi.org/10.1016/j.acra.2018.01.017.

[8] Y. Zhang, Y. Pan, T. Zhong, P. Dong, K. Xie, Y. Liu, H. Jiang, Z. Wu, Z. Liu, W. Zhao, W. Zhang, S. Zhao, T. Zhang, X. Jiang, D. Shen, T. Liu, and X. Zhang, "Potential of multimodal large language models for data mining of medical images and free-text reports," *Meta-Radiology*, vol. 2, no. 4, p. 100103, 2024, https://doi.org/10.1016/j.metrad.2024.100103.

[9] C. A. Andreucci, M. Martins, and C. A. Andreucci, "Mandibular fracture following dental implant protocol: Clinical report and one-year follow-up," *Osteology*, vol. 4, no. 1, pp. 1–10, 2024, https://doi.org/10.3390/osteology4010001.

[10] M. Ceddia, L. Lamberti, and B. Trentadue, "FEA comparison of the mechanical behavior of three dental crown materials: Enamel, ceramic, and zirconia," *Materials*, vol. 17, no. 3, p. 673, 2024, https://doi.org/10.3390/ma17030673.

[11] N. Tagliaferri, A. Pisciotta, G. Orlandi, G. Bertani, R. Di Tinco, L. Bertoni, P. Sena, A. Lunghi, M. Bianchi, F. Veneri, *et al.*, "Zirconia hybrid dental implants influence the biological properties of neural crest-derived mesenchymal stromal cells," *Nanomaterials*, vol. 14, no. 5, p. 392, 2024, https://doi.org/10.3390/nano14050392.

[12] M. A. Hasan, N. A. Abdullah, M. M. Rahman, M. Y. I. B. Idris, and O. F. Tawfiq, "Dental impression tray selection from maxillary arch images using multi-feature fusion and ensemble classifier," *IEEE Access*, vol. 9, pp. 30573–30586, 2021, https://doi.org/10.1109/ACCESS.2021.3059785.

[13] A. Bilal, A. H. Khan, K. Almohammadi, S. A. Al Ghamdi, H. Long, and H. Malik, "PDCNET: Deep convolutional neural network for classification of periodontal disease using dental radiographs," *IEEE Access*, vol. 12, pp. 150147–150168, 2024, https://doi.org/10.1109/ACCESS.2024.3472012.

[14] Z. Wu, Huangjian, and Zhengsong, "A feature selection and enhanced reuse framework for detection and classification of dental diseases in panoramic dental X-rays images," *IEEE Access*, vol. 13, pp. 70741–70751, 2025, https://doi.org/10.1109/ACCESS.2025.3561362.

[15] A. Imak, A. Celebi, K. Siddique, M. Turkoglu, A. Sengur, and I. Salam, "Dental caries detection using score-based multi-input deep convolutional neural network," *IEEE Access*, vol. 10, pp. 18320–18329, 2022, https://doi.org/10.1109/ACCESS.2022.3150358.

[16] R. Mladenovic, Z. Arsic, S. Velickovic, and M. Paunovic, "Assessing the efficacy of AI segmentation in diagnostics of nine supernumerary teeth in a pediatric patient," *Diagnostics*, vol. 13, no. 23, p. 3563, 2023, https://doi.org/10.3390/diagnostics13233563.

[17] X.-Y. Chen, G. Zhou, and J. Zhang, "Optical coherence tomography: Promising imaging technique for the diagnosis of oral mucosal diseases," *Oral Diseases*, vol. 30, no. 6, pp. 3638–3651, 2024, https://doi.org/10.1111/odi.14851.

[18] R. S. Jebur, M. H. B. M. Zabil, D. A. Hammood, and L. K. Cheng, "A comprehensive review of image denoising in deep learning," *Multimedia Tools and Applications*, vol. 83, no. 20, pp. 58181–58199, 2024, https://doi.org/10.1007/s11042-023-17468-2.

[19] K. Rahbar and F. Taheri, "Enhancing image retrieval through entropy-based deep metric learning," *Multimedia Tools and Applications*, vol. 84, no. 11, pp. 9065–9091, 2025, https://doi.org/10.1007/s11042-024-19296-4.

[20] W. Brahmi, I. Jdey, and F. Drira, "Exploring the role of convolutional neural networks (CNN) in dental radiography segmentation: A comprehensive systematic literature review," *Engineering Applications of Artificial Intelligence*, vol. 133, p. 108510, 2024, https://doi.org/10.1016/j.engappai.2024.108510.

[21] T.-Y. Su, J. C.-H. Wu, W.-C. Chiu, T.-J. Chen, W.-L. Lo, and H. H.-S. Lu, "Automatic classification of temporomandibular joint disorders by magnetic resonance imaging and convolutional neural networks," *Journal of Dental Sciences*, vol. 20, no. 1, pp. 393–401, 2025, https://doi.org/10.1016/j.jds.2024.06.001.

[22] Y.-N. Pang, Z. Yang, L.-X. Zhang, X.-Q. Liu, X.-S. Dong, X. Sheng, J.-G. Tan, X.-Y. Mao, and M.-Y. Liu, "Establishment and evaluation of a deep learning-based tooth wear severity grading system using intraoral photographs," *Journal of Dental Sciences*, vol. 20, no. 1, pp. 477–486, 2025, https://doi.org/10.1016/j.jds.2024.05.013.

[23] B. Tosun and Z. S. Yilmaz, "Comparison of artificial intelligence systems in answering prosthodontics questions from the dental specialty exam in Turkey," *Journal of Dental Sciences*, vol. 20, no. 3, pp. 1454–1459, 2025, https://doi.org/10.1016/j.jds.2025.01.025.

[24] K. D. Nguyen, H. T. Hoang, T.-P. H. Doan, K. Q. Dao, D.-H. Wang, and M.-L. Hsu, "SegmentAnyTooth: An open-source deep learning framework for tooth enumeration and segmentation in intraoral photos," *Journal of Dental Sciences*, vol. 20, no. 2, pp. 1110–1117, 2025, https://doi.org/10.1016/j.jds.2025.01.003.

[25] A.-Y. Su, M.-L. Wu, and Y.-H. Wu, "Deep learning system for the differential diagnosis of oral mucosal lesions through clinical photographic imaging," *Journal of Dental Sciences*, vol. 20, no. 1, pp. 54–60, 2025, https://doi.org/10.1016/j.jds.2024.10.019.

[26] N. Kyventidis and C. Angelopoulos, "Intraoral radiograph anatomical region classification using neural networks," *International Journal of Computer Assisted Radiology and Surgery*, vol. 16, no. 3, pp. 447–455, 2021, https://doi.org/10.1007/s11548-021-02321-4.

[27] T. Pankert, H. Lee, F. Peters, F. Hölzle, A. Modabber, and S. Raith, "Mandible segmentation from CT data for virtual surgical planning using an augmented two-stepped convolutional neural network," *International Journal of Computer Assisted Radiology and Surgery*, vol. 18, no. 8, pp. 1479–1488, 2023, https://doi.org/10.1007/s11548-022-02830-w.

[28] E. Halle, T. Amiel, D. J. Aframian, T. Malik, A. Rozenthal, O. Shauly, L. Joskowicz, C. Nadler, and T. Yeshua, "Automated segmentation and deep learning classification of ductopenic parotid salivary glands in sialo cone-beam CT images," *International Journal of Computer Assisted Radiology and Surgery*, vol. 20, no. 1, pp. 21–30, 2025, https://doi.org/10.1007/s11548-024-03240-w.

[29] W. H. Alawee, A. Basem, and L. A. Al-Haddad, "Advancing biomedical engineering: Leveraging Hjorth features for electroencephalography signal analysis," *Journal of Electrical Bioimpedance*, vol. 14, no. 1, pp. 66–72, 2023, https://doi.org/10.2478/joeb-2023-0009.

[30] L. A. Al-Haddad, W. H. Alawee, and A. Basem, "Advancing task recognition towards artificial limbs control with ReliefF-based deep neural network extreme learning," *Computers in Biology and Medicine*, vol. 169, p. 107894, 2024, https://doi.org/10.1016/j.compbiomed.2023.107894.

[31] Y. Zhang, F. Ye, L. Chen, F. Xu, X. Chen, H. Wu, M. Cao, Y. Li, Y. Wang, and X. Huang, "Children's dental panoramic radiographs dataset for caries segmentation and dental disease detection," *Scientific Data*, vol. 10, no. 1, p. 380, 2023, https://doi.org/10.1038/s41597-023-02237-5.

[32] H. Jiang, P. Zhang, C. Che, B. Jin, and Y. Zhu, "CariesFG: A fine-grained RGB image classification framework with attention mechanism for dental caries," *Engineering Applications of Artificial Intelligence*, vol. 123, p. 106306, 2023, https://doi.org/10.1016/j.engappai.2023.106306.

[33] J. Naidoo, S. C. Shelmerdine, C. F. U. Charcape, and A. S. Sodhi, "Artificial intelligence in paediatric tuberculosis," *Pediatric Radiology*, vol. 53, no. 9, pp. 1733–1745, 2023, https://doi.org/10.1007/s00247-023-05606-9.

[34] R. Ali, H. Li, J. R. Dillman, M. Altaye, H. Wang, N. A. Parikh, and L. He, "A self-training deep neural network for early prediction of cognitive deficits in very preterm infants using brain functional connectome data," *Pediatric Radiology*, vol. 52, no. 11, pp. 2227–2240, 2022, https://doi.org/10.1007/s00247-022-05510-8.

[35] J. R. Zech, D. Jaramillo, J. Altosaar, C. A. Popkin, and T. T. Wong, "Artificial intelligence to identify fractures on pediatric and young adult upper extremity radiographs," *Pediatric Radiology*, vol. 53, no. 12, pp. 2386–2397, 2023, https://doi.org/10.1007/s00247-023-05754-y.

[36] R. Bouali, O. Mahboub, and M. Lazaar, "Review of dental diagnosis by deep learning models: Trends, applications and challenges," *Procedia Computer Science*, vol. 231, pp. 221–228, 2024, https://doi.org/10.1016/j.procs.2023.12.196.

[37] R. C. Radha, B. S. Raghavendra, B. V. Subhash, J. Rajan, and A. V. Narasimhadhan, "Machine learning techniques for periodontitis and dental caries detection: A narrative review," *International Journal of Medical Informatics*, vol. 178, p. 105170, 2023, https://doi.org/10.1016/j.ijmedinf.2023.105170.

[38] S. Bhat, G. K. Birajdar, and M. D. Patil, "A comprehensive survey of deep learning algorithms and applications in dental radiograph analysis," *Healthcare Analytics*, vol. 4, p. 100282, 2023, https://doi.org/10.1016/j.health.2023.100282.

[39] A. Ramana Kumari, S. Nagaraja Rao, and P. Ramana Reddy, "Design of hybrid dental caries segmentation and caries detection with meta-heuristic-based ResNeXt-RNN," *Biomedical Signal Processing and Control*, vol. 78, p. 103961, 2022, https://doi.org/10.1016/j.bspc.2022.103961.

[40] M. Hamdan, Z. Badr, J. Bjork, R. Saxe, F. Malensek, C. Miller, R. Shah, S. Han, and H. Mohammad-Rahimi, "Detection of dental restorations using no-code artificial intelligence," *Journal of Dentistry*, vol. 139, p. 104768, 2023, https://doi.org/10.1016/j.jdent.2023.104768.

[41] W. M. Ahmed, A. A. Azhari, K. A. Fawaz, H. M. Ahmed, Z. M. Alsadah, A. Majumdar, and R. M. Carvalho, "Artificial intelligence in the detection and classification of dental caries," *The Journal of Prosthetic Dentistry*, vol. 133, no. 5, pp. 1326–1332, 2025, https://doi.org/10.1016/j.prosdent.2023.07.013.

[42] K. Yoon, H.-M. Jeong, J.-W. Kim, J.-H. Park, and J. Choi, "AI-based dental caries and tooth number detection in intraoral photos: Model development and performance evaluation," *Journal of Dentistry*, vol. 141, p. 104821, 2024, https://doi.org/10.1016/j.jdent.2023.104821.

[43] R. Esmaeilyfard, H. Bonyadifard, and M. Paknahad, "Dental caries detection and classification in CBCT images using deep learning," *International Dental Journal*, vol. 74, no. 2, pp. 328–334, 2024, https://doi.org/10.1016/j.identj.2023.10.003.

[44] A. A. Al Kheraif, A. A. Wahba, and H. Fouad, "Detection of dental diseases from radiographic 2D dental image using hybrid graph-cut technique and convolutional neural network," *Measurement*, vol. 146, pp. 333–342, 2019, https://doi.org/10.1016/j.measurement.2019.06.014.

[45] Y. Guo, J. Guo, Y. Li, P. Zhang, Y.-D. Zhao, Y. Qiao, B. Liu, and G. Wang, "Rapid detection of non-normal teeth on dental X-ray images using improved Mask R-CNN with attention mechanism," *International Journal of Computer Assisted Radiology and Surgery*, vol. 19, no. 4, pp. 779–790, 2024, https://doi.org/10.1007/s11548-023-03047-1.

[46] H. Chen, H. Li, Y. Zhao, J. Zhao, and Y. Wang, "Dental disease detection on periapical radiographs based on deep convolutional neural networks," *International Journal of Computer Assisted Radiology and Surgery*, vol. 16, no. 4, pp. 649–661, 2021, https://doi.org/10.1007/s11548-021-02319-y.

[47] L. A. Al-Haddad and A. A. Jaber, "Improved UAV blade unbalance prediction based on machine learning and ReliefF supreme feature ranking method," *Journal of the Brazilian Society of Mechanical Sciences and Engineering*, vol. 45, no. 9, p. 463, 2023, https://doi.org/10.1007/s40430-023-04386-5.

[48] J. Demšar and B. Zupan, "Orange: Data mining fruitful and fun—A historical perspective," *Informatica*, vol. 37, no. 1, pp. 55–60, 2013, https://www.informatica.si/index.php/informatica/article/view/434.

[49] F. A. Hashim, Y. M. Mohialden, and N. M. Hussien, "Hybrid feature selection and ensemble classification for climate change indicators: A machine learning approach," *Terra Joule Journal*, vol. 1, no. 2, p. 8, 2025, https://doi.org/10.64071/3080-5724.1021.

[50] M. I. Al-Karkhi, G. Rzadkowski, L. Ibraheem, and M. Aqib, "Anomaly detection in electrical systems using machine learning and statistical analysis," *Terra Joule Journal*, vol. 1, no. 2, p. 3, 2025, https://doi.org/10.64071/3080-5724.1012.

[51] L. A. Al-Haddad, L. Ibraheem, A. I. El-Seesy, A. A. Jaber, S. A. Al-Haddad, and R. Khosrozadeh, "Thermal heat flux distribution prediction in an electrical vehicle battery cell using finite element analysis and neural network," *Green Energy and Intelligent Transportation*, vol. 3, no. 3, p. 100155, 2024, https://doi.org/10.1016/j.geits.2024.100155.

[52] L. A. Al-Haddad, A. Jaber, L. Ibraheem, S. Al-Haddad, N. Ibrahim, and F. Abdulwahed, "Enhancing wind tunnel computational simulations of finite element analysis using machine learning-based algorithms," *Engineering and Technology Journal*, vol. 42, no. 1, pp. 135–143, 2024, https://doi.org/10.30684/etj.2023.142873.1552.

[53] M. Y. Fattah, L. A. Al-Haddad, M. Ayasrah, and A. A. Jaber, "Coupled finite element and artificial neural network analysis of interfering strip footings in saturated cohesive soils," *Transportation Infrastructure Geotechnology*, vol. 11, no. 4, pp. 2168–2185, 2024, https://doi.org/10.1007/s40515-023-00369-0.

[54] L. A. Al-Haddad, A. Łukaszewicz, H. S. Majdi, A. Holovatyy, A. A. Jaber, M. I. Al-Karkhi, and W. Giernacki, "Energy consumption and efficiency degradation predictive analysis in unmanned aerial vehicle batteries using deep neural networks," *Advances in Science and Technology Research Journal*, vol. 19, no. 5, pp. 21–30, 2025, https://doi.org/10.12913/22998624/201346.

[55] L. A. Al-Haddad, H. A. H. Kahachi, H. Z. Ur Rehman, A. A. Al-Zubaidi, M. I. Al-Karkhi, and B. Al-Oubaidi, "Advancing sustainability in buildings using an integrated aerodynamic façade: Potential of artificial intelligence," *Terra Joule Journal*, vol. 1, no. 1, pp. 1–9, 2025, https://doi.org/10.64071/3080-5724.1006.

[56] M. Hung, M. W. Voss, M. N. Rosales, W. Li, W. Su, J. Xu, J. Bounsanga, B. Ruiz-Negrón, E. Lauren, and F. W. Licari, "Application of machine learning for diagnostic prediction of root caries," *Gerodontology*, vol. 36, no. 4, pp. 395–404, Dec. 2019, https://doi.org/10.1111/ger.12432.

[57] N. Shiota, A. Kinoshita, M. Sunaga, G. Tanabe, K. Hayashi, H. Churei, T. Fukai, M. Matsumoto, T. Yasui, and T. Ueno, "Effectiveness of computer-assisted learning in sports dentistry: Studies over a

multiple-year period and at two universities," *European Journal of Dental Education*, vol. 25, no. 4, pp. 796–805, Nov. 2021, https://doi.org/10.1111/eje.12659.

[58] X. Zhang, Y. Liang, W. Li, C. Liu, D. Gu, W. Sun, and L. Miao, "Development and evaluation of deep learning for screening dental caries from oral photographs," *Oral Diseases*, vol. 28, no. 1, pp. 173–181, Jan. 2022, https://doi.org/10.1111/odi.13735.

[59] D. R. Nayak, R. Dash, B. Majhi, and Y. Zhang, "A hybrid regularized extreme learning machine for automated detection of pathological brain," *Biocybernetics and Biomedical Engineering*, vol. 39, no. 3, pp. 880–892, Jul. 2019, https://doi.org/10.1016/j.bbe.2019.08.005.

[60] M. Nahiduzzaman, M. O. Faruq Goni, M. R. Islam, A. Sayeed, M. S. Anower, M. Ahsan, J. Haider, and M. Kowalski, "Detection of various lung diseases including COVID-19 using extreme learning machine algorithm based on the features extracted from a lightweight CNN architecture," *Biocybernetics and Biomedical Engineering*, vol. 43, no. 3, pp. 528–550, Jul. 2023, https://doi.org/10.1016/j.bbe.2023.06.003.

[61] S. A. Sarow, H. A. Flayyih, M. Bazerkan, L. A. Al-Haddad, Z. T. Al-Sharify, and A. A. F. Ogaili, "Advancing sustainable renewable energy: XGBoost algorithm for the prediction of water yield in hemispherical solar stills," *Discover Sustainability*, vol. 5, no. 1, p. 510, Dec. 2024, https://doi.org/10.1007/s43621-024-00782-6.

[62] A. R. K. Jweri, L. A. Al-Haddad, A. Ogaili, A. Jaber, and M. I. Al-Karkhi, "Edge-intelligent leak detection in water distribution systems using CatBoost: A sustainable solution for reducing infrastructure losses," *Clean Energy Science and Technology*, vol. 3, no. 4, pp. 1–28, Oct. 2025, https://doi.org/10.18686/cest398.

[63] B. G. Mejbel, S. A. Sarow, M. T. Al-Sharify, L. A. Al-Haddad, A. A. F. Ogaili, and Z. T. Al-Sharify, "A data fusion analysis and random forest learning for enhanced control and failure diagnosis in rotating machinery," *Journal of Failure Analysis and Prevention*, vol. 24, no. 6, pp. 2979–2989, Dec. 2024, https://doi.org/10.1007/s11668-024-02075-6.

[64] A. A. F. Ogaili, N. T. Al-Sharify, Z. T. Al-Sharify, M. T. Al-Sharify, A. A. Jaber, and E. Z. Gheni, "Temporal feature extraction and gradient boosting for binary cardiac acoustic classification," in *Data Science and Communication Engineering*, D. Misra, M. Chakraborty, D. De, and R. Buyya, Eds. Singapore: Springer Nature Singapore, 2025, pp. 443–459, https://doi.org/10.1007/978-981-96-4543-5_31.

[65] L. Nassir, A. Ramadhan, N. Al-Sharify, M. Khalaf, A. Ogaili, A. Jaber, and Z. T. Al-Sharify, "Robust multi-state EEG cognitive classification via optimized time-domain features and CatBoost," *International Journal of Robotics and Control Systems*, vol. 5, no. 2, pp. 968–989, 2025, https://doi.org/10.31763/ijrcs.v5i2.1799.

[66] L. A. Al-Haddad and A. A. Jaber, "An intelligent fault diagnosis approach for multirotor UAVs based on deep neural network of multi-resolution transform features," *Drones*, vol. 7, no. 2, p. 82, 2023, https://doi.org/10.3390/drones7020082.

[67] A. S. Abdul-Zahra, E. Ghane, A. Kamali, and A. A. F. Ogaili, "Power forecasting in continuous extrusion of pure titanium using naïve Bayes algorithm," *Terra Joule Journal*, vol. 1, no. 1, p. 2, 2025, https://doi.org/10.64071/3080-5724.1000.

[68] A. A. F. Ogaili, Z. T. Al-Sharify, A. A. Jaber, D. A. Farhan, and S. M. Al-Khafaji, "Effective ball bearing fault diagnosis leveraging ANN and statistical feature integration," in *CEUR Workshop Proceedings*, pp. 42–48, 2025, https://ceur-ws.org/Vol-3870/p06.pdf.

[69] A. R. K. Jweri, A. A. F. Ogaili, S. A. Amin, M. I. Khalaf, L. A. Al-Haddad, A. A. Jaber, and M. I. Al-Karkhi, "Enhancing predictive maintenance in energy systems using a hybrid Kolmogorov-Arnold network (KAN) with short-time Fourier transform (STFT) framework for rotating machinery," *ASEAN Journal of Science and Engineering*, vol. 5, no. 2, pp. 465–494, 2025, https://doi.org/10.17509/ajse.v5i2.89023.

[70] S. T. Bunyan, Z. H. Khan, L. A. Al-Haddad, H. A. Dhahad, M. I. Al-Karkhi, A. A. F. Ogaili, and Z. T. Al-Sharify, "Intelligent thermal condition monitoring for predictive maintenance of gas turbines using machine learning," *Machines*, vol. 13, no. 5, p. 401, 2025, https://doi.org/10.3390/machines13050401.